

# Hollow vortex problem in a wedge and the associated Riemann-Hilbert problem on a torus\*

Y.A. ANTIPOV AND A.Y. ZEMLYANOVA

Department of Mathematics, Louisiana State University  
Baton Rouge, LA 70803, USA

Department of Mathematics, Kansas State University  
Manhattan, KS 66506, USA

## Abstract

Reconstruction of conformal mappings from canonical slit domains onto multiply-connected physical domains with a free boundary is of interest in many different models arising in fluid mechanics and elasticity. In the present paper, an exact formula for the conformal map from the exterior of two slits onto the doubly connected flow domain is obtained when a fluid flows in a wedge about a hollow vortex. The map is expressed in terms of a rational function on an elliptic surface topologically equivalent to a torus and the solution to a symmetric Riemann-Hilbert problem on a finite and a semi-infinite segments on the same Riemann surface. Owing to its special features, the Riemann-Hilbert problem requires a novel analogue of the Cauchy kernel on an elliptic surface. Such a kernel is proposed, its properties are studied, and it is employed to derive a closed-form solution to the Riemann-Hilbert problem. The solution procedure also includes the solution to the associated Jacobi inversion problem and a transcendental equation for the conformal mapping parameters. The final formula for the conformal map possesses a free parameter, and a one-parametric family of hollow vortices in a wedge is constructed.

## 1 Introduction

A hollow vortex is defined as a region of a fluid bounded by a vortex sheet with the fluid in the interior of this region being at rest with respect to the frame of reference. This implies that the hollow vortex boundary is a streamline, and pressure on the boundary is constant. Analysis of flow of a fluid about hollow vortices requires determining free vortices' boundaries and therefore solving nonlinear inverse problems. First studies [23, 20] of hollow vortices were published at the end of the nineteenth century. In particular, Pocklington [23] studied a two-dimensional problem of uniform flow of a fluid with a pair of hollow vortices of the same area and the circulations of opposite signs.

To date, there is only a limited number of exact solutions concerning flows about hollow vortices. A review of such solutions which had been published by the beginning of the nineties was given in [25]. One of the solutions [8] concerns the problem on a linear array of hollow vortices in an inviscid incompressible fluid when each vortex has a fore-and-aft symmetry. The problem was solved by the method of conformal mappings, and the solution was employed to study the stability of the flow. It turns out that if a ratio of the vortex area to the square of the separation distance is less than a certain critical value, then two different vortex shapes exist. Moreover, vortices with more deformed boundaries become unstable. The kinetic energy of the array [8] of hollow vortices was investigated in [7]. The exact solution of the problem of a double street of vortices with vortex

---

\*The research was partly supported by EPSRC grant no EP/R014604/1 and the Simons Foundation grants no. 319217 and 713080.

patches or point vortices instead of hollow vortices was obtained in [26]. Hollow vortices could be used [16] to model wakes behind bluff bodies in liquid flows. This idea was utilized to describe various flows of liquid [18, 29, 14].

Smith and Crowdy [28] studied a single two-dimensional hollow vortex in linear and non-linear straining flows of different orders at infinity. The stability of the single hollow vortex was examined and a new type of resonance-induced instability was identified. The method of conformal mappings was applied [10] to solve the problem [26] of two infinite rows of hollow vortices. The conformal map was written in terms of the Schottky-Klein prime function. This special function was also applied to solve the problem of a translating pair of symmetric opposite and equal finite cross-section hollow vortices [11] and the problem of co-travelling hollow vortices in a channel [15]. A hollow vortex in a pure shear flow was studied in [30]. The stagnation points of Pocklington's hollow vortex flow were replaced [31] by Chaplygin cusps which are the regions of fluid at rest. The method of a hodograph plane and conformal mappings was utilized and the classical Pocklington solutions were generalized to flows inside channels.

Generalizations of hollow vortices with uniform vorticity known as Sadovskii's vortices [24] were examined in [22]. An array of Sadovskii's vortices was considered and its stability was analyzed in [27]. Equilibrium configurations of several co-rotating uniform vortices and stability of the vortex configuration were inspected and energy of the vortex array was computed in [13]. Stability issues of the polygonal arrays of uniform vortices were studied in [12]. Analysis of motion of uniform vortex patches shows [9] that  $m$ -fold symmetric hypotrochoid vortex patches are exact steady solutions when rotation and strain are present.

Several studies extended the hollow vortex problems in incompressible fluid to compressible fluid including [17, 21], where a self-propagating pair of vortices of equal and opposite strength in an inviscid compressible liquid was examined. The Rayleigh-Janzen approximation was used [6] to solve the problem of a single row of hollow vortices in a compressible liquid by enhancing the corresponding incompressible solution.

The present study concerns the problem of motion of a fluid about a hollow vortex in a wedge with impenetrable walls. Unlike [28], in this case, the order of the flow at infinity cannot be taken arbitrarily and is completely determined by the wedge angle. Another crucial difference is that the flow domain is doubly-connected, not simply-connected as in [28]. The problem is exactly solved by constructing the conformal mapping from the exterior of two cuts,  $l_0 = [m, \infty)$  and  $l_1 = [0, 1]$ , onto the flow domain. Here,  $m$  is a free parameter, and  $m > 1$ . The semi-infinite cut is mapped onto the boundary of the wedge, the wedge vertex is the image of some point  $a$  on the lower side of the contour  $l_0$ , whilst the finite cut is mapped onto the boundary of the hollow vortex. The conformal mapping is presented in terms of two functions. One of them is a rational function on an elliptic surface  $\mathcal{R}$  topologically equivalent to a torus. The second one is the solution to a symmetric Riemann-Hilbert problem on the Riemann surface  $\mathcal{R}$ . Solutions to Riemann-Hilbert problems on genus-0, elliptic and hyperelliptic Riemann surfaces were used [2, 3, 4, 5, 32] to reconstruct the conformal mappings associated with supercavitating flows in simply and multiply-connected domains. It turns out that the Weierstrass analogue of the Cauchy kernel [33] employed in these studies of supercavitating flows is not applicable to the Riemann-Hilbert problem arising in the hollow vortex problem in a wedge. The reason is that the Weierstrass kernel is not sufficiently decaying at infinity with respect to the variable of integration, and its use leads to divergent integrals. We propose a new analogue of the Cauchy kernel on a hyperelliptic surface with the properties needed. In the elliptic case, this kernel has simple poles at two bounded points of the surface. These poles generate unacceptable essential singularities of the factorization function. They are removed by solving the associated Jacobi inversion problem. The factorization of the coefficient of the Riemann-Hilbert problem is used further to derive the general solution to the Riemann-Hilbert problem that possesses a rational function on the surface  $\mathcal{R}$ . By satisfying

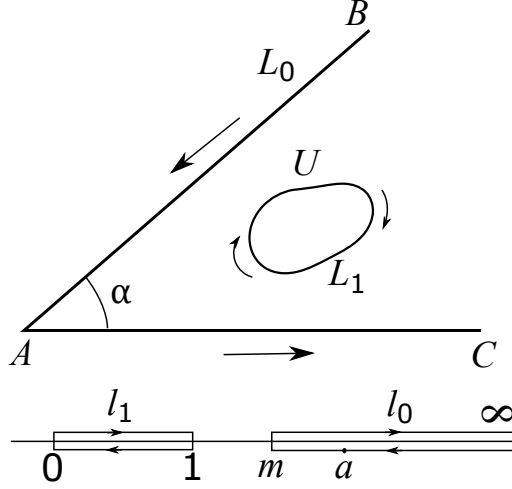


Figure 1: Geometry of the model. Physical and parametric domains.

the additional conditions we arrive at a real transcendental equation with respect to two real parameters, the preimage  $a$  of the wedge vertex and the parameter  $m$ . This gives rise to a one-parametric family of conformal mappings associated with the problem.

This paper is organized as follows. In Section 2, we state the problem of a hollow vortex in a wedge and express the conformal map through two functions,  $\omega_0(\zeta)$  and  $\omega_1(\zeta)$ . In Section 3, we determine the function  $\omega_0(\zeta)$ . We derive and solve the Riemann-Hilbert problem on the elliptic surface  $\mathcal{R}$  for the function  $\omega_1(\zeta)$  in Section 4. The exact formula for the conformal map is presented in Section 5. We employ this map to reconstruct the hollow vortex and the wedge boundaries and report the numerical results in Section 6.

## 2 Model problem formulation and a conformal mapping

We consider two-dimensional flow of an inviscid incompressible fluid in a wedge  $W$  around a hollow vortex  $L_1$  located inside the wedge (Fig.1). The wedge boundary  $L_0$  is formed by rigid walls  $AC = \{z \in \mathbb{C} : z = x > 0\}$  and  $AB = \{z \in \mathbb{C} : z = re^{i\alpha}, r > 0, 0 < \alpha < 2\pi\}$ . The flow exterior to the vortex is irrotational and characterized by a complex potential  $w(z) = \phi(x, y) + i\psi(x, y)$  whose derivative describes the velocity vector  $\mathbf{v} = (u, v)$  by  $dw/dz = u - iv$ ,  $z \in \tilde{\mathcal{D}} = W \setminus \text{int}(L_1)$ . Here,  $\phi$  is the velocity potential,  $\psi$  is the stream function,  $z = x + iy$ , and  $\tilde{\mathcal{D}}$  is the flow domain. The potential  $w(z)$  is an analytic multi-valued function in the flow domain with a cyclic period (the circulation about the vortex)  $\Gamma$ ,

$$\int_{L_1} \frac{dw}{dz} dz = \Gamma, \quad (2.1)$$

and satisfies the following boundary conditions. On the wedge walls they are

$$\arg \frac{dw}{dz} = \begin{cases} \pi - \alpha, & z \in AB, \\ 0, & z \in AC, \end{cases} \quad \text{Im } w = c_0 = \text{const}, \quad z \in L_0. \quad (2.2)$$

The boundary  $L_1$  of the hollow vortex is a streamline,  $\psi(x, y) = c_1 = \text{const}$ ,  $z \in L_1$ . In addition, on  $L_1$ , the flow speed  $|dw/dz|$  is constant and prescribed. Thus the boundary conditions on the vortex boundary read

$$\text{Im } w = c_1, \quad \left| \frac{dw}{dz} \right| = U, \quad z \in L_1. \quad (2.3)$$

At large distances, the complex potential behaves as

$$w(z) \sim \frac{\Gamma}{2\pi i} \log z + Cz^\beta, \quad z \rightarrow \infty, \quad z \in \tilde{\mathcal{D}}, \quad (2.4)$$

where  $\beta > 0$  is a parameter to be determined, and  $C$  is a constant.

Consider another complex plane, a  $\zeta$ -plane, cut along two segments,  $l_0 = [m, +\infty)$  ( $m > 1$ ) and  $l_1 = [0, 1]$ . Denote the exterior of these two slits by  $\mathcal{D}$ . Let  $z = f(\zeta)$  be a conformal map of this doubly connected domain onto the flow domain  $\tilde{\mathcal{D}}$ . We assume that the function  $f(\zeta)$  maps the slits  $l_0$  and  $l_1$  onto the wedge and vortex boundaries  $L_0$  and  $L_1$ , respectively. The positive directions of the contours  $l_0$  and  $l_1$  are chosen such that when a point  $\zeta$  traverses the contours, the domain  $\mathcal{D}$  is left on the left. For the upper and lower sides of the contours  $l_0$  and  $l_1$ , we shall use the notations  $l_0^\pm$  and  $l_1^\pm$ , respectively. We choose the map such that the infinite point  $\zeta = \infty \in \mathcal{D}$  falls into the infinite point of the flow domain,  $z = \infty \in \tilde{\mathcal{D}}$ . Without loss, it is assumed that the preimage of the wedge vertex  $A$  is a point  $a$  lying in the lower side of the semi-infinite cut,  $a \in [m, +\infty)^-$ . This assumption inevitably gives us the preimages of the points  $B$  and  $C$  in the parametric plane: they are  $+\infty - i0$  and  $+\infty + i0$ , respectively.

In order to reconstruct the conformal mapping, we express the derivative  $f'(\zeta)$  through the derivative  $dw/d\zeta$  and the logarithmic hodograph variable as

$$\frac{df}{d\zeta} = \omega_0(\zeta)e^{-\omega_1(\zeta)}, \quad (2.5)$$

where

$$\omega_0(\zeta) = \frac{dw}{Ud\zeta}, \quad \omega_1(\zeta) = \log \frac{dw}{Udz}. \quad (2.6)$$

### 3 Function $\omega_0(\zeta)$ and asymptotics of the map

Since the imaginary part of the function  $w(z)$  is constant on  $L_0$  and  $L_1$ , we have  $\text{Im } dw/d\zeta = 0$  on the contours  $l_0$  and  $l_1$ . In virtue of (2.6) the function  $\omega_0(\zeta)$  is analytic in the domain  $\mathcal{D} = \mathbb{C} \setminus (l_0 \cup l_1)$ , satisfies the boundary condition

$$\text{Im } \omega_0(\xi) = 0, \quad \xi \in l_0 \cup l_1, \quad (3.1)$$

and may have integrable singularities at the finite endpoints of the contours  $l_0$  and  $l_1$ . At infinity,  $\omega_0(\zeta) = O(\zeta^{-\mu})$  with  $\mu > 0$ . The most general form of such a function is

$$\omega_0(\zeta) = \frac{i(N_0 + N_1\zeta)}{p^{1/2}(\zeta)}, \quad (3.2)$$

where  $N_0$  and  $N_1$  are arbitrary real constants, and

$$p(\zeta) = \zeta(1 - \zeta)(\zeta - m). \quad (3.3)$$

The function  $p^{1/2}(\zeta)$  is analytic in the  $\zeta$ -plane cut along the lines  $l_0$  and  $l_1$ . Its single branch is fixed by the condition  $p^{1/2}(\zeta) = i\sqrt{|p(\xi)|}$  as  $\zeta = \xi + i0$ ,  $\xi > m$ . This branch has the following properties:

$$p^{1/2}(\zeta) = \pm i\sqrt{|p(\xi)|}, \quad \zeta = \xi \pm i0, \quad m < \xi < +\infty,$$

$$p^{1/2}(\zeta) = -\sqrt{|p(\xi)|}, \quad \zeta = \xi, \quad 1 < \xi < m,$$

$$p^{1/2}(\zeta) = \mp i\sqrt{|p(\xi)|}, \quad \zeta = \xi \pm i0, \quad 0 < \xi < 1,$$

$$p^{1/2}(\zeta) = \sqrt{|p(\xi)|}, \quad \zeta = \xi, \quad -\infty < \xi < 0. \quad (3.4)$$

The function  $\omega_0(\zeta)$  is bounded as  $\zeta \rightarrow a$  if  $a \neq m$  and has the square root singularity  $\omega_0(\zeta) = O((\zeta - a)^{-1/2})$  otherwise.

We next analyze the behavior of the function  $f(\zeta)$  at the points  $\zeta = a$  and  $\zeta = \infty$ . Consider a copy of the  $\zeta$ -plane cut along the semi-infinite segment  $l_0 = [m, \infty)$ . By the map  $f_1(\zeta) = \sqrt{\zeta - m}$  it is transformed into the upper half-plane with the points  $m$  and  $a \in l_0^-$  being transformed into the origin and the point  $-\sqrt{a - m}$ , respectively. By the translation transformation  $f_2(\zeta) = f_1(\zeta) + \sqrt{a - m}$  we move the point  $-\sqrt{a - m}$  into the origin. Finally, by implementing the transformation  $z = f_2^{\alpha/\pi}(\zeta)$ , we map the upper half-plane into the wedge  $W$  in the  $z$ -plane. The composition of these three maps has the form

$$z = (\sqrt{\zeta - m} + \sqrt{a - m})^{\alpha/\pi} = \frac{(\zeta - a)^{\alpha/\pi}}{(\sqrt{\zeta - m} - \sqrt{a - m})^{\alpha/\pi}}. \quad (3.5)$$

Note that this map transforms the finite cut  $l_1$  into a closed contour inside the wedge  $W$ . The map (3.5) and the function  $f(\zeta)$  share the same asymptotics at the points  $a$  and  $\infty$ . Consequently, if  $a \neq m$ , then formula (3.5) implies

$$\begin{aligned} f(\zeta) &\sim K_0(\zeta - a)^{\alpha/\pi}, \quad \zeta \rightarrow a \in l_0^-, \quad f(\zeta) \sim K_1, \quad \zeta \rightarrow \bar{a} \in l_0^+, \\ f(\zeta) &\sim \zeta^{\alpha/(2\pi)}, \quad \zeta \rightarrow \infty. \end{aligned} \quad (3.6)$$

Here,  $K_0$  and  $K_1$  are some constants.

In the case  $a = m$ , the asymptotics of the function  $f(\zeta)$  at infinity is the same, whilst at the left endpoint of the cut  $l_0$ , we have

$$f(\zeta) \sim K_0(\zeta - a)^{\alpha/(2\pi)}, \quad \zeta \rightarrow a = m. \quad (3.7)$$

## 4 Function $\omega_1(\zeta)$ and a Riemann-Hilbert problem on a torus

### 4.1 Hilbert problem for the function $\omega_1(\zeta)$

We now turn our attention to the function  $\omega_1(\zeta)$ . Comparing the asymptotics (2.4) and (3.6) at infinity and using formula (3.2) we deduce from (2.5) and (2.6)

$$\beta = \frac{\pi}{\alpha}, \quad \frac{dw}{Udz} \sim \frac{\pi C}{\alpha} \zeta^{(\pi - \alpha)/(2\pi)}, \quad \zeta \rightarrow \infty, \quad (4.1)$$

and therefore

$$\omega_1(\zeta) \sim \frac{\pi - \alpha}{2\pi} \log \zeta, \quad \zeta \rightarrow \infty. \quad (4.2)$$

In a similar fashion we determine the asymptotics of the function  $\omega_1(\zeta)$  at the point  $a$ . If  $a \neq m$  ( $a \in l_0^-$ ), then we have

$$\frac{dw}{Udz} \sim C'(\zeta - a)^{1 - \alpha/\pi}, \quad \zeta \rightarrow a, \quad \frac{dw}{Udz} \sim C'', \quad \zeta \rightarrow \bar{a}, \quad (4.3)$$

where  $C'$  and  $C''$  are constants. The second formula in (2.6) yields

$$\omega_1(\zeta) \sim \frac{\pi - \alpha}{\pi} \log(\zeta - a), \quad \zeta \rightarrow a, \quad \omega_1(\zeta) \sim \log C'', \quad \zeta \rightarrow \bar{a}. \quad (4.4)$$

If it happens that  $a = m$ , then

$$\omega_1(\zeta) \sim \frac{\pi - \alpha}{2\pi} \log(\zeta - a), \quad \zeta \rightarrow a. \quad (4.5)$$

At the point  $\bar{a}$  the function  $\omega_1(\zeta)$  is bounded and at infinity has the same asymptotics (4.2) as in the case  $a \neq m$ .

Analyze next the boundary conditions. Observe in equations (2.2) and (2.3) that the values of the argument and modulus of the function  $dw/dz$  give rise to the imaginary and real parts of the function  $\omega_1(\zeta)$ . We have

$$\operatorname{Im} \omega_1(\zeta) = \begin{cases} \pi - \alpha, & \zeta \in l'_0, \\ 0, & \zeta \in l''_0, \end{cases} \quad \operatorname{Re} \omega_1(\zeta) = 0, \quad \zeta \in l_1. \quad (4.6)$$

Here,  $l'_0 = [a, +\infty)^-$ ,  $l''_0 = [m, a]^- \cup [m, +\infty)^+$ , and the superscripts  $+$  and  $-$  indicate that the segments belong to the upper and lower sides of the contour  $l_0$ , correspondingly. The problem for the function  $\omega_1(\zeta)$  obtained is classified as a Hilbert problem of the theory of analytic functions on two two-sided positively oriented contours (the exterior of the loops  $l_0$  and  $l_1$  is on the left when a point  $\zeta$  traverses the contours in the positive direction). To solve this problem, we reduce it to a Riemann-Hilbert problem on two contours of a symmetric genus-1 Riemann surface topologically equivalent to a torus.

#### 4.2 Riemann-Hilbert problem for an auxiliary function $\Phi(\zeta, u)$ on a torus

Let  $\mathbb{C}_1$  and  $\mathbb{C}_2$  be two copies of the extended complex  $\zeta$ -plane cut along the segments  $l_1 = [0, 1]$  and  $l_0 = [m, +\infty)$  and  $\mathcal{R}$  be a genus-1 Riemann surface defined by the algebraic equation

$$u^2 = p(\zeta), \quad p(\zeta) = \zeta(1 - \zeta)(\zeta - m). \quad (4.7)$$

The surface is formed by gluing the two sheets together in such a way that the upper sides  $l_j^+$  of the cuts  $l_j \subset \mathbb{C}_1$  are glued to the lower sides  $l_j^-$  of the cuts  $l_j \subset \mathbb{C}_2$ , and the sides  $l_j^- \subset \mathbb{C}_1$  are glued to  $l_j^+ \subset \mathbb{C}_2$  ( $j = 0, 1$ ). Let  $p^{1/2}(\zeta)$  be the branch fixed in Section 3. Then the function  $u(\zeta)$

$$u = \begin{cases} p^{1/2}(\zeta), & (\zeta, u) \in \mathbb{C}_1, \\ -p^{1/2}(\zeta), & (\zeta, u) \in \mathbb{C}_2, \end{cases} \quad (4.8)$$

is uniquely defined and single-valued on  $\mathcal{R}$ . The pairs  $(\zeta, p^{1/2}(\zeta))$  and  $(\zeta, -p^{1/2}(\zeta))$  correspond to the points with affix  $\zeta$  lying on the upper and lower sheets,  $\mathbb{C}_1$  and  $\mathbb{C}_2$ , respectively. The contour  $\mathcal{L} = l_0 \cup l_1$  is the symmetry line for the elliptic surface  $\mathcal{R}$  which splits the surface into two symmetric halves with symmetric points  $(\zeta, u) \in \mathbb{C}_1$  and  $(\zeta_*, u_*) = (\bar{\zeta}, -u(\bar{\zeta})) \in \mathbb{C}_2$ .

Introduce an auxiliary function on the surface  $\mathcal{R}$

$$\Phi(\zeta, u) = \begin{cases} -i\omega_1(\zeta), & (\zeta, u) \in \mathbb{C}_1, \\ i\overline{\omega_1(\bar{\zeta})}, & (\zeta, u) \in \mathbb{C}_2. \end{cases} \quad (4.9)$$

Everywhere on the torus this function satisfies the symmetry condition

$$\overline{\Phi(\zeta_*, u_*)} = \Phi(\zeta, u), \quad (\zeta, u) \in \mathcal{R}. \quad (4.10)$$

On the symmetry line  $\mathcal{L}$ , its boundary values are expressed through the real and imaginary values of the function  $\omega_1(\xi)$ ,

$$\begin{aligned} \Phi^+(\xi, v) &= -i\omega_1(\xi) = -i \operatorname{Re} \omega_1(\xi) + \operatorname{Im} \omega_1(\xi), \\ \Phi^-(\xi, v) &= i\overline{\omega_1(\xi)} = i \operatorname{Re} \omega_1(\xi) + \operatorname{Im} \omega_1(\xi), \quad (\xi, v) \in \mathcal{L}, \quad v = u(\xi), \end{aligned} \quad (4.11)$$

where  $\Phi^+(\xi, v)$  ( $\Phi^-(\xi, v)$ ) is the limiting value of the function  $\Phi(\zeta, u)$  on the contour  $\mathcal{L}$  from the upper (lower) sheet of the surface. On summarizing the properties of the function  $\Phi(\zeta, u)$  we state to the following Riemann-Hilbert problem.

Find all symmetric functions  $\Phi(\zeta, u)$ ,  $\overline{\Phi(\zeta_*, u_*)} = \Phi(\zeta, u)$ ,  $(\zeta, u) \in \mathcal{R}$ , analytic in  $\mathcal{R} \setminus \mathcal{L}$ , Hölder-continuous up to the boundary  $\mathcal{L}$  apart from the singular points  $\zeta = a$  and  $\zeta = \infty$  with the boundary values satisfying the relation

$$\Phi^+(\xi, v) = G(\xi, v)\Phi^-(\xi, v) + g(\xi, v), \quad (\xi, v) \in \mathcal{L}, \quad (4.12)$$

Here,

$$G(\xi, v) = \begin{cases} -1, & (\xi, v) \in l_0 \\ 1, & (\xi, v) \in l_1, \end{cases} \quad g(\xi, v) = \begin{cases} 2(\pi - \alpha), & (\xi, v) \in l'_0, \\ 0, & (\xi, v) \in l''_0, \\ 0, & (\xi, v) \in l_1. \end{cases} \quad (4.13)$$

The function  $\Phi(\zeta, u)$  has a logarithmic singularity at the infinite point  $(\infty, \infty)$ ,

$$\Phi(\zeta, u) \sim \frac{\pi - \alpha}{2\pi i} \log \zeta, \quad \zeta \rightarrow \infty, \quad (4.14)$$

It is bounded at the point  $(\bar{a}, u(\bar{a}))$  and has a logarithmic singularity at the point  $(a, u(a))$ ,

$$\Phi(\zeta, u) \sim \frac{\pi - \alpha}{\sigma\pi i} \log(\zeta - a), \quad \zeta \rightarrow a, \quad (4.15)$$

where  $\sigma = 1$  if  $a \neq m$  and  $\sigma = 2$  otherwise.

### 4.3 Analogue of the Cauchy kernel

The standard solution device for scalar Riemann-Hilbert problems on elliptic and hyperelliptic surfaces is the Wierstrass kernel [33], an analogue of the Cauchy kernel for Riemann surfaces. It has the form

$$dW = \frac{1}{2} \left( 1 + \frac{u}{v} \right) \frac{d\xi}{\xi - \zeta}, \quad u = u(\zeta), \quad v = u(\xi). \quad (4.16)$$

This kernel is applicable if the Riemann-Hilbert problem contour is bounded or the density decays at infinity at a sufficient rate otherwise. When the contour is unbounded and the density does not decay at infinity fast enough, the employment of the kernel (4.16) gives rise to divergent integrals. In our case the contour  $\mathcal{L}$  of the Riemann-Hilbert problem comprises a finite contour  $l_1$  and a semi-infinite contour  $l_0$ . Since the function  $g(\xi, v)$  defined in (4.13) is a nonzero constant in the contour  $l'_0 = [a, \infty)^-$ , we need a kernel different from the one in (4.16).

We propose to use a new analogue of the Cauchy kernel convenient for our purposes. Consider the differential

$$dV = \frac{1}{2} \left[ 1 + \frac{u(\xi - \zeta_0)^2}{v(\zeta - \zeta_0)^2} \right] \left( \frac{1}{\xi - \zeta} - \frac{1}{\xi - \zeta_0} \right) d\xi, \quad (4.17)$$

where  $\zeta_0$  is an arbitrary fixed point of the surface not lying on the contours  $l_0$  and  $l_1$ . Equivalently, the kernel  $dV$  may be written in the form

$$dV = \frac{1}{2} \left[ \frac{\zeta - \zeta_0}{\xi - \zeta_0} + \frac{u}{v} \frac{\xi - \zeta_0}{\zeta - \zeta_0} \right] \frac{d\xi}{\xi - \zeta}. \quad (4.18)$$

Since the kernel needs to be symmetric, we select  $\zeta_0$  to be real and not lying in the contours  $l_0$  and  $l_1$ . Let  $\zeta_0$  be an arbitrary negative number. This kernel possesses the following properties.

(i) If  $\zeta$  is a fixed bounded point on the torus  $\mathcal{R}$  and  $\xi \rightarrow \pm i0 + \infty$ , then  $dV$  is decaying as  $\xi^{-3/2}$  that is

$$dV \sim \pm \frac{1}{2i} \frac{u(\zeta)}{\zeta - \zeta_0} \xi^{-3/2} d\xi, \quad \xi \rightarrow \pm i0 + \infty. \quad (4.19)$$

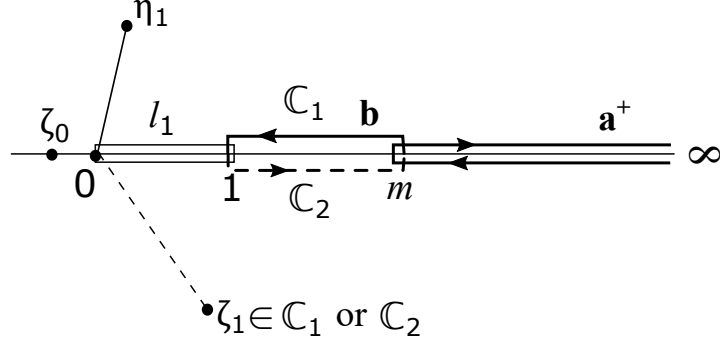


Figure 2: Canonical cross-sections and the contour  $\gamma = \mathbf{p}_1 \mathbf{q}_1$ ,  $\mathbf{p}_1 = (\eta_1, u(\eta_1)) \in \mathbb{C}_1$ , and  $\mathbf{q}_1 = (\zeta_1, u(\zeta_1)) \in \mathcal{R}$ .

(ii) If  $\xi$  is a fixed point lying either in the contour  $l_1$  or any finite part of the contour  $l_0$  and  $\zeta \rightarrow \infty$ , then the kernel  $dV$  is bounded,

$$dV \sim \left[ -\frac{1}{2(\xi - \zeta_0)} + O(\zeta^{-1/2}) \right] d\xi, \quad \zeta \rightarrow \infty. \quad (4.20)$$

(iii) If  $\zeta \rightarrow \xi \in \mathcal{L}$ , then the kernel behaves as the Cauchy kernel. Indeed, if  $\zeta \in \mathbb{C}_1$  and  $\zeta \rightarrow \xi$ , then for  $\xi \in \mathcal{L} \subset \mathbb{C}_1$

$$dV \sim \frac{d\xi}{\xi - \zeta}, \quad (4.21)$$

whilst for  $\xi \in \mathcal{L} \subset \mathbb{C}_2$ ,  $u/v \sim -1$ , and the kernel  $dV$  is bounded. The analysis is similar when  $\zeta \in \mathbb{C}_2$ .

(iv) Since  $\zeta_0$  is a real number, the kernel  $dV$  is symmetric with respect to the symmetry contour  $\mathcal{L}$ ,

$$dV((\xi, v), (\zeta, u(\zeta))) = \overline{dV((\xi, v), (\bar{\zeta}, -u(\bar{\zeta})))}. \quad (4.22)$$

(v) At the two points of the torus with affix  $\zeta_0$ ,  $(\zeta_0, u(\zeta_0))$  and  $(\zeta_0, -u(\zeta_0))$ , the kernel  $dV$  has simple poles. They will give rise to essential singularities of the factorization problem associated with the Riemann-Hilbert problem (4.12) and will have to be removed by solving a Jacobi inversion problem.

#### 4.4 Factorization problem

We aim to determine a piece-wise meromorphic function  $X(\zeta, u)$  symmetric on the torus,

$$X(\zeta, u) = \overline{X(\bar{\zeta}, -u(\bar{\zeta}))}, \quad (\zeta, u) \in \mathcal{R} \setminus \mathcal{L}, \quad (4.23)$$

continuous through the contour  $l_1$ , discontinuous through the contour  $l_0$ , and whose boundary values on the contour satisfy the equation

$$X^+(\xi, v) = G(\xi, v) X^-(\xi, v), \quad (\xi, v) \in \mathcal{L} \subset \mathcal{R}. \quad (4.24)$$

Analyze the following function:

$$X(\zeta, u) = \chi(\zeta, u) \chi_1(\zeta, u) \overline{\chi_1(\zeta_*, u_*)}, \quad (4.25)$$

where

$$\chi(\zeta, u) = \exp \left\{ \frac{1}{2\pi i} \oint_{l_0} \log(-1) dV \right\},$$



$$\chi_1(\zeta, u) = \exp \left\{ - \left( \int_{\gamma} + n_a \oint_{\mathbf{a}} + n_b \oint_{\mathbf{b}} \right) dV \right\}. \quad (4.26)$$

The contours  $\mathbf{a}$  and  $\mathbf{b}$  constitute a system of canonical cross-sections of the surface  $\mathcal{R}$ . They are chosen as follows. The contour  $\mathbf{a}$  lies on both sheets of the surface and coincides with the banks of the semi-infinite cut  $l_0$  (Fig.2). The loop  $\mathbf{b}$  consists of the segments  $[m, 1] \subset \mathbb{C}_1$  and  $[1, m] \subset \mathbb{C}_2$ . The positive direction on the loop  $\mathbf{a}$  is chosen such that the upper sheet is on the left. The loop  $\mathbf{a}$  intersects the loop  $\mathbf{b}$  at the branch point  $\zeta = m$  from left to the right.

The contour  $\gamma$  is a continuous curve whose starting and terminal points are  $\mathbf{p}_1 = (\eta_1, u(\eta_1))$  and  $\mathbf{q}_1 = (\zeta_1, u(\zeta_1))$ , respectively. The point  $\mathbf{p}_1$  is an arbitrary fixed point lying in either sheet of the surface. Without loss, select  $\mathbf{p}_1 = (\eta_1, p^{1/2}(\eta_1)) \in \mathbb{C}_1$ . As for the point  $\mathbf{q}_1$ , it has to be determined and may fall on either sheet. The integers  $n_a$  and  $n_b$  cannot be fixed *a priori* either and are to be recovered from a condition which guarantees the boundedness of the solution to the problem (4.24) at the two points of the torus with affix  $\zeta_0$ , the simple poles of the kernel  $dV$ . The contour  $\gamma$  is chosen such that it does not cross the  $\mathbf{a}$ - and  $\mathbf{b}$ -cross-sections. In the case  $\mathbf{q}_1 \in \mathbb{C}_2$ , it passes through the point  $\zeta = 0$ , a branch point of the surface  $\mathcal{R}$ , and consists of two parts,  $(\mathbf{p}_1, 0) \subset \mathbb{C}_1$  and  $(0, \mathbf{q}_1) \subset \mathbb{C}_2$ . If it turns out that the point  $\mathbf{q}_1$  lies on the upper sheet, then the contour  $\gamma$  can be taken as the straight segment joining these points provided it does not cross the loops  $l_0$  and  $l_1$ . Otherwise, if the imaginary parts of the points  $\eta_1$  and  $\zeta_1$  have different signs, both points  $\mathbf{p}_1$  and  $\mathbf{q}_1$  lie in the sheet  $\mathbb{C}_1$ , and the straight segment  $\mathbf{p}_1\mathbf{q}_1$  intersects the contour  $\mathcal{L}$ , then  $\gamma$  can be selected as a polygonal line consisting of two segments  $\mathbf{p}_1\mathbf{p}_0$  and  $\mathbf{p}_0\mathbf{q}_1$  with  $\mathbf{p}_0 = (\delta, p^{1/2}(\delta))$  and  $\zeta_0 < \delta < 0$ .

Note that the integrals in (4.26) have jumps through the contours  $\gamma$ ,  $\mathbf{a}$ , and  $\mathbf{b}$ , respectively. However, since the jumps are multiples of  $2\pi i$ , the functions in the right hand-side in (4.25) are continuous through these contours. It is directly verified that the function (4.25) satisfies the symmetry condition (4.23).

The integral representation of the factorization function  $X(\zeta, u)$  can be simplified. By employing the Cauchy theorem we deduce

$$\chi(\zeta, u) = \exp \left\{ \frac{u(\zeta)}{4(\zeta - \zeta_0)} \oint_{l_0} \frac{(\xi - \zeta_0)d\xi}{u(\xi)(\xi - \zeta)} \right\}. \quad (4.27)$$

In the product  $\chi_1(\zeta, u)\overline{\chi_1(\zeta_*, u_*)}$ , the integrals over the cross-section  $\mathbf{b}$  are cancelled and we deduce

$$\begin{aligned} \chi_1(\zeta, u)\overline{\chi_1(\zeta_*, u_*)} &= \exp \left\{ -\frac{1}{2} \int_{\gamma} \left( \frac{\zeta - \zeta_0}{\xi - \zeta_0} + \frac{u(\zeta)}{u(\xi)} \frac{\xi - \zeta_0}{\zeta - \zeta_0} \right) \frac{d\xi}{\xi - \zeta} \right. \\ &\quad \left. - \frac{1}{2} \int_{\gamma} \left( \frac{\zeta - \zeta_0}{\bar{\xi} - \zeta_0} - \frac{u(\zeta)}{u(\bar{\xi})} \frac{\bar{\xi} - \zeta_0}{\zeta - \zeta_0} \right) \frac{d\bar{\xi}}{\bar{\xi} - \zeta} - \frac{n_a u(\zeta)}{\zeta - \zeta_0} \oint_{\mathbf{a}} \frac{(\xi - \zeta_0)d\xi}{u(\xi)(\xi - \zeta)} \right\}. \end{aligned} \quad (4.28)$$

Since the contour  $l_0$  and the loop  $\mathbf{a}$  have the same direction and coincide pointwise, we derive the following representation for the solution of the factorization problem:

$$\begin{aligned} X(\zeta, u) &= \exp \left\{ \left( \frac{1}{2} - 2n_a \right) \frac{u(\zeta)}{i(\zeta - \zeta_0)} \int_m^\infty \frac{(\xi - \zeta_0)d\xi}{\sqrt{|p(\xi)|}(\xi - \zeta)} \right. \\ &\quad \left. - \frac{1}{2} \int_{\gamma} \left( \frac{\zeta - \zeta_0}{\xi - \zeta_0} + \frac{u(\zeta)}{u(\xi)} \frac{\xi - \zeta_0}{\zeta - \zeta_0} \right) \frac{d\xi}{\xi - \zeta} - \frac{1}{2} \int_{\gamma} \left( \frac{\zeta - \zeta_0}{\bar{\xi} - \zeta_0} - \frac{u(\zeta)}{u(\bar{\xi})} \frac{\bar{\xi} - \zeta_0}{\zeta - \zeta_0} \right) \frac{d\bar{\xi}}{\bar{\xi} - \zeta} \right\}. \end{aligned} \quad (4.29)$$

We describe the main properties of the function  $X(\zeta, u)$  given by (4.29).

(i) The function  $X(\zeta, u)$  satisfies the symmetry condition (4.23) and the boundary condition (4.24).

(ii) The limit values  $X^+(\xi \pm i0, u^\pm(\xi))$  and  $X^-(\xi \pm i0, u^\pm(\xi))$  on both sides of the contour  $l_0$  are expressed through the Cauchy principal value of the first integral in (4.29) as

$$\begin{aligned} X^+(\xi \pm i0, u^\pm(\xi)) &= iX(\xi, u^\pm(\xi)), \quad \xi \in l_0^\pm. \\ X^-(\xi \pm i0, u^\pm(\xi)) &= -iX(\xi, u^\pm(\xi)), \quad \xi \in l_0^\pm. \end{aligned} \quad (4.30)$$

(iii) In virtue of the behavior of the Cauchy integral at the endpoints of the contour  $\gamma$ , the function  $X(\zeta, u)$  has a simple zero at the point  $\mathbf{p}_1 \in \mathbb{C}_1$  and a simple pole at the point  $\mathbf{q}_1 \in \mathcal{R}$ .

(iv) As a consequence of the poles of the kernel at the points  $(\zeta_0, u(\zeta_0))$  and  $(\zeta_0, -u(\zeta_0))$ , the function  $X(\zeta, u)$  has essential singularities at these two points. They will be removed in the next section by solving a certain Jacobi inversion problem.

#### 4.5 Jacobi inversion problem

To remove the essential singularities of the factorization function  $X(\zeta, u)$  at the points  $(\zeta_0, \pm u(\zeta_0))$ , we require

$$\operatorname{res}_{\zeta=\zeta_0} \frac{u(\zeta)}{\zeta - \zeta_0} \left\{ \left( \frac{1}{2} - 2n_a \right) \int_m^\infty \frac{(\xi - \zeta_0)d\xi}{i\sqrt{|p(\xi)|}(\xi - \zeta)} - \frac{1}{2} \int_\gamma \frac{(\xi - \zeta_0)d\xi}{u(\xi)(\xi - \zeta)} + \frac{1}{2} \int_\gamma \frac{(\bar{\xi} - \zeta_0)d\bar{\xi}}{u(\bar{\xi})(\bar{\xi} - \zeta)} \right\} = 0. \quad (4.31)$$

This brings us to the following nonlinear equation with respect to the point  $\mathbf{q}_1$ , the terminal point of the contour  $\gamma$ , and the integer  $n_a$ :

$$\left( \frac{1}{4} - n_a \right) \oint_{\mathbf{a}} \frac{d\xi}{u(\xi)} - \frac{1}{2} \int_\gamma \frac{d\xi}{u(\xi)} + \frac{1}{2} \int_\gamma \frac{d\bar{\xi}}{u(\bar{\xi})} = 0, \quad (4.32)$$

which can be considered [4] as an imaginary analogue of the Jacobi inversion problem

$$\int_0^{\mathbf{q}_1} \frac{d\xi}{u(\xi)} + n_a \mathcal{A} + n_b \mathcal{B} = g_0, \quad (4.33)$$

where  $\mathcal{A}$  and  $\mathcal{B}$  are the  $\mathcal{A}$ - and  $\mathcal{B}$ - periods of the abelian integral

$$\int_0^{\mathbf{q}} \frac{d\xi}{u(\xi)} \quad (4.34)$$

given in terms of the Legendre complete elliptic integrals [19]

$$\begin{aligned} \mathcal{A} &= \oint_{\mathbf{a}} \frac{d\xi}{u(\xi)} = -2i \int_m^\infty \frac{d\xi}{\sqrt{|\xi(\xi-1)(\xi-m)|}} = -4ik\mathbf{K}(k), \\ \mathcal{B} &= \oint_{\mathbf{b}} \frac{d\xi}{u(\xi)} = 2 \int_1^m \frac{d\xi}{\sqrt{|\xi(\xi-1)(\xi-m)|}} = 4k\mathbf{K}'(k), \end{aligned} \quad (4.35)$$

$k = m^{-1/2}$ , and

$$g_0 = -ik\mathbf{K}(k) + \int_0^{n_1} \frac{d\xi}{p^{1/2}(\xi)}. \quad (4.36)$$

The only one difference between the Jacobi problem (4.33) and the one solved in [4] is the right hand-side  $g_0$ . By adjusting the formulas [4] to our case we can describe the solution procedure as follows. Compute the affix of the point  $\mathbf{q}_1$  by

$$\zeta_1 = \operatorname{sn}^2 \frac{ig_0}{2k} \quad (4.37)$$

and evaluate the integrals

$$I_{\pm} = \int_0^{\eta_1} \frac{d\xi}{p^{1/2}(\xi)} \pm \int_0^{\zeta_1} \frac{d\xi}{p^{1/2}(\xi)} - ik\mathbf{K}(k) \quad (4.38)$$

and the numbers  $n_a$  and  $n_b$

$$n_a = -\frac{\operatorname{Im} I_-}{4k\mathbf{K}(k)}, \quad n_b = \frac{\operatorname{Re} I_-}{4k\mathbf{K}'(k)}. \quad (4.39)$$

If both of the numbers  $n_a$  and  $n_b$  are integers, then the point  $\mathbf{q}_1$  lies in the upper sheet  $\mathbb{C}_1$ ,  $\mathbf{q}_1 = (\zeta_1, p^{1/2}(\zeta_1))$ . Otherwise,  $\mathbf{q}_1 \in \mathbb{C}_2$ ,  $\mathbf{q}_1 = (\zeta_1, -p^{1/2}(\zeta_1))$ , and the numbers  $n_a$  and  $n_b$  computed by the formulas

$$n_a = -\frac{\operatorname{Im} I_+}{4k\mathbf{K}(k)}, \quad n_b = \frac{\operatorname{Re} I_+}{4k\mathbf{K}'(k)} \quad (4.40)$$

are integers. If the point  $\mathbf{q}_1$  and the integer  $n_a$  are evaluated according to this procedure, then the function  $X(\zeta, u)$  is bounded at the points  $(\zeta_0, \pm u(\zeta_0))$  and provides a solution to the factorization problem (4.23), (4.24).

#### 4.6 Solution to the Riemann-Hilbert problem

First we use the factorization of the function  $G(\xi, v)$  and rewrite the boundary condition (4.12) in the form

$$\frac{\Phi^+(\xi, v)}{X^+(\xi, v)} = \frac{\Phi^-(\xi, v)}{X^-(\xi, v)} + \frac{g(\xi, v)}{X^+(\xi, v)}, \quad (\xi, v) \in \mathcal{L}. \quad (4.41)$$

Next we introduce the singular integral with the kernel  $dV$  on the torus  $\mathcal{R}$

$$\Psi(\zeta, u) = \frac{\pi - \alpha}{2\pi i} \int_{l'_0} \left[ \frac{\zeta - \zeta_0}{\xi - \zeta_0} + \frac{u(\zeta)}{u(\xi)} \frac{\xi - \zeta_0}{\zeta - \zeta_0} \right] \frac{d\xi}{(\xi - \zeta)X^+(\xi, u(\xi))}. \quad (4.42)$$

Note that this function satisfies the symmetry condition  $\Psi(\zeta, u) = \overline{\Psi(\zeta_*, u_*)}$ , is discontinuous through the contour  $l'_0$  with the jump  $2(\pi - \alpha)/X^+(\xi, v)$  and continuous through the contours  $l''_0$  and  $l_1$ .

We apply the Sokhotski-Plemelj formulas, the continuity principle and the generalized Liouville theorem on the torus  $\mathcal{R}$  to deduce the general solution to the Riemann-Hilbert problem (4.12)

$$\Phi(\zeta, u) = X(\zeta, u)[\Psi(\zeta, u) + \Omega(\zeta, u)], \quad (\zeta, u) \in \mathcal{R}. \quad (4.43)$$

Here,  $\Omega(\zeta, u)$  is a rational function on the torus  $\mathcal{R}$ . It possesses the following properties.

(i) Since the kernel  $dV$  has simple poles at the points  $(\zeta_0, \pm u(\zeta_0))$  on both sheets of the surface  $\mathcal{R}$ , the function  $\Psi(\zeta, u)$  has simple poles at these points. This gives simple poles to the function  $\Phi(\zeta, u)$  which are unacceptable. To remove them, we admit that the function  $\Omega(\zeta, u)$  also has simple poles at the points  $(\zeta_0, \pm u(\zeta_0))$  and require that

$$\operatorname{res}_{\zeta=\zeta_0} [\Psi(\zeta, u) + \Omega(\zeta, u)] = 0. \quad (4.44)$$

(ii) Owing to the simple pole of the function  $X(\zeta, u)$  at the point  $\mathbf{q}_1 = (\zeta_1, u(\zeta_1)) \in \mathcal{R}$ , the function  $\Psi(\zeta, u) + \Omega(\zeta, u)$  vanishes at this point,

$$\Psi(\zeta_1, u(\zeta_1)) + \Omega(\zeta_1, u(\zeta_1)) = 0. \quad (4.45)$$

(iii) Because of the simple zero of the function  $X(\zeta, u)$  at the point  $\mathbf{p}_1 = (\eta_1, u(\eta_1)) \in \mathbb{C}_1$ , the function  $\Omega(\zeta, u)$  has a simple pole at this point.

(iv) Since the functions  $X(\zeta, u)$  and  $\Psi(\zeta, u)$  are bounded at infinity and the function  $\Phi(\zeta, u)$  has to be bounded, the function  $\Omega(\zeta, u)$  must be bounded as  $\zeta \rightarrow \infty$  as well.

(v) Owing to the symmetry of the functions  $\Phi(\zeta, u)$ ,  $X(\zeta, u)$ , and  $\Psi(\zeta, u)$ , the function  $\Omega(\zeta, u)$  is also symmetric,  $\Omega(\zeta, u) = \overline{\Omega(\zeta_*, u_*)}$ .

The most general form of such a rational function is

$$\begin{aligned} \Omega(\zeta, u) = & M_0 + (M_1 + iM_2) \frac{u(\zeta) + u(\eta_1)}{\zeta - \eta_1} - (M_1 - iM_2) \frac{u(\zeta) - u(\bar{\eta}_1)}{\zeta - \bar{\eta}_1} \\ & + (M_3 + iM_4) \frac{u(\zeta) + u(\zeta_0)}{\zeta - \zeta_0} - (M_3 - iM_4) \frac{u(\zeta) - u(\bar{\zeta}_0)}{\zeta - \bar{\zeta}_0}, \end{aligned} \quad (4.46)$$

where  $M_j$  ( $j = 0, 1, \dots, 4$ ) are arbitrary real constants. This function satisfies the conditions (iii) and (v). Because of the growth of the function  $u(\zeta)$  at infinity as  $\zeta^{3/2}$ , in general, the function  $\Omega(\zeta, u)$  is unbounded at infinity. It becomes bounded and the condition (iv) is satisfied if

$$M_2 = -M_4. \quad (4.47)$$

To fulfill the property (i), that is to meet the condition (4.44), define the constants  $M_3$  and  $M_4$  as

$$M_3 = 0, \quad M_4 = \frac{\pi - \alpha}{4\pi} \int_{l'_0} \frac{d\xi}{u(\xi)X^+(\xi, v)}. \quad (4.48)$$

Finally, we make sure that the rational function  $\Omega(\zeta, u)$  has property (ii). Denote

$$\begin{aligned} R + iJ = & \Psi(\zeta_1, u(\zeta_1)), \quad R_0 + iJ_0 = \frac{2u(\zeta_1)}{\zeta_1 - \zeta_0}, \\ R_1 + iJ_1 = & \frac{u(\zeta_1) + u(\eta_1)}{\zeta_1 - \eta_1}, \quad R_2 + iJ_2 = \frac{u(\zeta_1) - u(\bar{\eta}_1)}{\zeta_1 - \bar{\eta}_1}. \end{aligned} \quad (4.49)$$

where  $R$ ,  $J$ ,  $R_l$ , and  $J_l$  ( $l = 0, 1, 2$ ) are real. Then equation (4.45) implies

$$M_1 = \frac{(R_0 - R_1 - R_2)M_2 - J}{J_1 - J_2},$$

$$M_0 = (R_2 - R_1)M_1 + (J_1 + J_2 - J_0)M_2 - R. \quad (4.50)$$

Having uniquely obtained all the five constants  $M_j$  ( $j = 0, 1, \dots, 4$ ) in the rational function  $\Omega(\zeta, u)$ , we simplify it as

$$\Omega(\zeta, u) = M_0 + (M_1 + iM_2) \frac{u(\zeta) + u(\eta_1)}{\zeta - \eta_1} - (M_1 - iM_2) \frac{u(\zeta) - u(\bar{\eta}_1)}{\zeta - \bar{\eta}_1} - \frac{2iM_2u(\zeta)}{\zeta - \zeta_0} \quad (4.51)$$

and complete the solution procedure for the Riemann-Hilbert problem (4.12) by analyzing the behavior of the function  $\Phi(\zeta, u)$  at the points  $a$  and  $\infty$ .

Analysis of the integral  $\Psi(\zeta, u)$  with the kernel  $dV$  as  $\zeta \rightarrow a$  and  $\zeta \rightarrow \bar{a}$  yields

$$\Psi(\zeta, u) \sim \frac{\pi - \alpha}{\sigma\pi i X^+(a, u(a))} \log(\zeta - a), \quad \zeta \rightarrow a, \quad \Psi(\zeta, u) \sim \text{const}, \quad \zeta \rightarrow \bar{a}, \quad (4.52)$$

where  $\sigma = 1$  when  $a \neq m$  and  $\sigma = 2$  otherwise. Here, we took into account that the starting and terminal points of the contour  $l_0''$  are  $+\infty - i0$  and  $a \in l_0^-$ , respectively. Therefore, in virtue of (4.43), the function  $\Phi(\zeta, u)$  has the logarithmic singularity, as  $\zeta \rightarrow a$ , and its asymptotics coincides with (4.15) predicted by employing formulas (2.5) and (2.6) and implementing asymptotic analysis of the conformal map  $z = f(\zeta)$  in Section 3. As  $\zeta \rightarrow \bar{a}$ , the function  $\Phi(\zeta, u)$  is bounded.

Analyze next the behavior of the functions  $\Psi(\zeta, u)$  and  $\Phi(\zeta, u)$  at infinity. By making the substitutions  $\tau = 1/\xi$ ,  $t = 1/\zeta$  we deduce as  $\zeta \in l_0' = (a, +\infty)^-$ ,

$$\Psi^+\left(\frac{1}{t}, u\left(\frac{1}{t}\right)\right) = \frac{\pi - \alpha}{X^+(1/t, u^-(1/t))} + \frac{\pi - \alpha}{2\pi i}(\mathcal{I}_1 + \mathcal{I}_2), \quad (4.53)$$

where

$$\begin{aligned} \mathcal{I}_1 &= \int_0^{1/a} \frac{1 - t\zeta_0}{1 - \tau\zeta_0} \frac{d\tau}{(\tau - t)X^+(1/\tau, u^-(1/\tau))}, \\ \mathcal{I}_2 &= \int_0^{1/a} \sqrt{\frac{t(1-t)(1-mt)}{\tau(1-\tau)(1-m\tau)}} \frac{1 - \tau\zeta_0}{1 - t\zeta_0} \frac{d\tau}{(\tau - t)X^+(1/\tau, u^-(1/\tau))}. \end{aligned} \quad (4.54)$$

As  $t \rightarrow 0$  and  $\zeta \in l_0'$ , the integral  $\mathcal{I}_2$  is bounded, whilst the integral  $\mathcal{I}_1$  has a logarithmic singularity, and we have

$$\Psi^+(\zeta, u) \sim \frac{\pi - \alpha}{2\pi i X^+(+\infty - i0, v)} \log \zeta, \quad \zeta \rightarrow +\infty - i0. \quad (4.55)$$

It turns out that the principal term of the asymptotics of the function  $\Psi(\zeta, u)$  as  $\zeta \rightarrow +\infty + i0$  along the contour  $l_0''$  is the same as in (4.55). In virtue of formula (4.43) we discover that  $\Phi(\zeta, u) \sim (\pi - \alpha)/(2\pi i) \log \zeta$  as  $\zeta \rightarrow \infty$  along the contour  $l_0$ . This formula is identical to the asymptotics (4.14) obtained before by means of the asymptotic analysis of the conformal mapping in Section 3.

## 5 Exact representation of the conformal mapping $z = f(\zeta)$

The conformal mapping from the parametric domain  $\mathcal{D}$  onto the flow domain  $\tilde{\mathcal{D}}$  is given by

$$f(\zeta) = i \int_a^\zeta \frac{N_0 + iN_1\xi}{p^{1/2}(\xi)} e^{-i\Phi^+(\xi, u(\xi))} d\xi, \quad \zeta \in \mathcal{D}, \quad (5.1)$$

The solution obtained has to satisfy two extra equations, the circulation condition (2.1) and the complex equation

$$\int_{l_1} \frac{df}{d\zeta} d\zeta = 0 \quad (5.2)$$

which guarantees that the conformal mapping is single-valued. Owing to formulas (2.5) and (2.6) we transform the circulation condition (2.1) into the form

$$\int_0^1 \frac{(N_0 + N_1\xi)d\xi}{\sqrt{|p(\xi)|}} = -\frac{\Gamma}{2U}. \quad (5.3)$$

This integral can be computed and expressed through the complete elliptic integrals of the first and second kind. We have

$$\begin{aligned} \int_0^1 \frac{d\xi}{\sqrt{|p(\xi)|}} &= 2k\mathbf{K}(k), \\ \int_0^1 \frac{\xi d\xi}{\sqrt{|p(\xi)|}} &= \frac{2}{k}[\mathbf{K}(k) - \mathbf{E}(k)], \quad k = \frac{1}{\sqrt{m}}. \end{aligned} \quad (5.4)$$

On substituting the integrals (5.4) into equation (5.3) we obtain a relation between the two real constants  $N_0$  and  $N_1$ ,

$$N_0 = -\frac{1}{k\mathbf{K}(k)} \left[ \frac{\Gamma}{4U} + \frac{\mathbf{K}(k) - \mathbf{E}(k)}{k} N_1 \right]. \quad (5.5)$$

Transform now the second condition, equation (5.2). On substituting the representation (5.1) into equation (5.2) and denoting

$$c^\pm(\xi) = \cos[\Phi^+(\xi, u^\pm(\xi))], \quad s^\pm(\xi) = \sin[\Phi^+(\xi, u^\pm(\xi))], \quad \xi \in l_1^\pm, \quad (5.6)$$

we write equation (5.2) in the form

$$\begin{aligned} N_0 \int_0^1 \frac{c^+(\xi) + c^-(\xi) - is^+(\xi) - is^-(\xi)}{\sqrt{|p(\xi)|}} d\xi \\ + N_1 \int_0^1 \frac{c^+(\xi) + c^-(\xi) - is^+(\xi) - is^-(\xi)}{\sqrt{|p(\xi)|}} \xi d\xi = 0. \end{aligned} \quad (5.7)$$

Note that since  $\text{Im } \Phi^+(\xi, u^\pm(\xi)) = 0$  on  $l_0^\pm$ , the functions  $c^\pm(\xi)$  and  $s^\pm(\xi)$  are real-valued. On taking the real and imaginary parts of equation (5.7) we deduce

$$N_0 C_0 + N_1 C_1 = 0 \quad (5.8)$$

and

$$C_0 S_1 - C_1 S_0 = 0. \quad (5.9)$$

Here,

$$C_j = \int_0^1 \frac{c^+(\xi) + c^-(\xi)}{\sqrt{|p(\xi)|}} \xi^j d\xi, \quad S_j = \int_0^1 \frac{s^+(\xi) + s^-(\xi)}{\sqrt{|p(\xi)|}} \xi^j d\xi, \quad j = 0, 1. \quad (5.10)$$

Thus, in addition to equation (5.5) we obtained another equation for the constants  $N_0$  and  $N_1$  and we have

$$N_0 = - \left[ 1 - \frac{\mathbf{K}(k) - \mathbf{E}(k)}{k^2 \mathbf{K}(k)} \frac{C_0}{C_1} \right]^{-1} \frac{\Gamma}{4Uk\mathbf{K}(k)}, \quad N_1 = -\frac{N_0 C_0}{C_1}. \quad (5.11)$$

Equation (5.9) is a real transcendental equation for the two real parameters  $a$  and  $m$ . This enables us to conclude that the original problem possesses a one-parametric family of solutions provided equation (5.9) has a solution and it is unique.

## 6 Reconstruction of the hollow vortex and the wedge boundaries and numerical results

The first step of the numerical procedure is to select a value of the parameter  $m$  and determine the parameter  $a$  by solving the transcendental equation (5.9). At this stage, we need to evaluate the integrals (5.10) whose integrands depend on the solution  $\Phi^+(\xi, u)$  on the contour  $l_1$  and are independent of the constants  $N_0$  and  $N_1$ . The function  $\Phi^+(\xi, u)$  is given by (4.43) in terms of the factorization function  $X(\zeta, u)$ , the integral  $\Psi(\zeta, u)$ , and the rational function  $\Omega(\zeta, u)$ . The factorization function depends on the point  $\mathbf{q}_1$  and the integer  $n_a$ , the solution to the Jacobi inversion problem. It turns out that for all realistic values of the problem parameters used in the numerical tests and when  $\mathbf{p}_1 = (\eta_1, u(\eta_1)) \in \mathbb{C}_1$ ,  $\eta_1 = i$ , the point  $\mathbf{q}_1 = (\zeta_1, u(\zeta_1))$  also lies in the upper sheet  $\mathbb{C}_1$ , and  $n_a = 0$ .

It is convenient to write the function  $X(\zeta, u)$  in the form

$$X(\zeta, u) = \lambda \exp \left\{ \frac{u(\zeta, u)}{i(\zeta - \zeta_0)} \left( \frac{1}{2} - 2n_a \right) \mathcal{J}_1(\zeta) - \frac{\mathcal{J}_2(\zeta, u) + \mathcal{J}_3(\zeta, u)}{2} \right\}, \quad (6.1)$$

where  $\lambda = 1$  if  $(\zeta, u) \in \mathbb{C}_1 \setminus l_0$ ,  $\lambda = i(-1)^{j-1}$  if  $(\zeta, u) \in l_0 \subset \mathbb{C}_j$ ,  $j = 1, 2$ ,

$$\begin{aligned}\mathcal{J}_1(\zeta) &= \int_m^\infty \frac{(\xi - \zeta_0)d\xi}{\sqrt{\xi(\xi-1)(\xi-m)}(\xi-\zeta)}, \\ \mathcal{J}_2(\zeta, u) &= \int_\gamma \left( \frac{\zeta - \zeta_0}{\xi - \zeta_0} + \frac{u(\zeta)}{u(\xi)} \frac{\xi - \zeta_0}{\zeta - \zeta_0} \right) \frac{d\xi}{\xi - \zeta}, \\ \mathcal{J}_3(\zeta, u) &= \int_\gamma \left( \frac{\zeta - \zeta_0}{\bar{\xi} - \zeta_0} - \frac{u(\zeta)}{u(\xi)} \frac{\bar{\xi} - \zeta_0}{\zeta - \zeta_0} \right) \frac{d\bar{\xi}}{\bar{\xi} - \zeta}.\end{aligned}\quad (6.2)$$

Analyze the first integral. If  $\zeta \notin (m, +\infty)$ , by making the substitution  $\xi = 1/\tau$  we obtain

$$\mathcal{J}_1(\zeta) = \frac{1}{\sqrt{m}} \int_0^{1/m} \frac{\mathcal{F}_1(\tau)d\tau}{\sqrt{\tau(1/m-\tau)}}, \quad \mathcal{F}_1(\tau) = \frac{1 - \zeta_0\tau}{\sqrt{1-\tau(1-\tau\zeta)}}. \quad (6.3)$$

By employing the integration formula with the Gaussian weights  $\pi/n$  and abscissas  $x_j = \cos(j - \frac{1}{2})\frac{\pi}{n}$  we write approximately

$$\mathcal{J}_1(\zeta) \approx \frac{\pi}{\sqrt{mn}} \sum_{j=1}^n \mathcal{F}_1\left(\frac{1+x_j}{2m}\right). \quad (6.4)$$

When  $\zeta \in (m, +\infty)$ , the integral  $\mathcal{J}_1(\zeta)$  is singular, and its Cauchy principal value is computed by [1]

$$\mathcal{J}_1(\zeta) = -\frac{2\pi\sqrt{m}}{\zeta} \sum_{s=1}^\infty d'_s U_{s-1}\left(\frac{2m}{\zeta} - 1\right), \quad (6.5)$$

where

$$\begin{aligned}d'_s &= \frac{2}{\pi} \int_{-1}^1 \tilde{\mathcal{F}}_1\left(\frac{1+\tau}{2m}\right) \frac{T_s(\tau)d\tau}{\sqrt{1-\tau^2}} \approx \frac{2}{n} \sum_{j=1}^n \tilde{\mathcal{F}}_1\left(\frac{1+x_j}{2m}\right) \cos\left(j - \frac{1}{2}\right) \frac{s\pi}{n}, \quad s = 1, 2, \dots \\ \tilde{\mathcal{F}}_1(\tau) &= \frac{1 - \tau\zeta_0}{\sqrt{1-\tau}},\end{aligned}\quad (6.6)$$

and  $T_s(\tau)$  are the Chebyshev polynomials of the first kind. Since all the numerical tests result in  $\text{Im } \zeta_1 \text{Im } \eta_1 < 0$ , we split the contour  $\gamma$  into two segments  $(\eta_1, \delta)$  and  $(\delta, \zeta_1)$ ,  $\zeta_0 < \delta < 0$  lying in the upper sheet. This leads to the following representations of the integrals  $\mathcal{J}_2$  and  $\mathcal{J}_3$ :

$$\mathcal{J}_2(\zeta, u) = j^+(\zeta, u; \zeta_1) - j^+(\zeta, u; \eta_1), \quad \mathcal{J}_3(\zeta, u) = j^-(\zeta, u; \bar{\zeta}_1) - j^-(\zeta, u; \bar{\eta}_1), \quad (6.7)$$

where

$$j^\pm(\zeta, u; \eta) = \int_\delta^\eta \left( \frac{\zeta - \zeta_0}{\xi - \zeta_0} \pm \frac{u(\zeta)}{u(\xi)} \frac{\xi - \zeta_0}{\zeta - \zeta_0} \right) \frac{d\xi}{\xi - \zeta}. \quad (6.8)$$

The last integrals are not singular, and both of the Simpson rule and the Gauss quadrature formula provide numerical values with a good accuracy.

Consider next the function  $\Psi(\zeta, u)$ . If  $\zeta \notin l'_0 = (a, +\infty)^-$ , then the integral is not singular. On making the substitution  $\xi = 1/\tau$ , we recast it as

$$\Psi(\zeta, u) = -\frac{\pi - \alpha}{2\pi i} \int_0^{1/a} \frac{\mathcal{F}_*(\zeta, u; \tau)d\tau}{\sqrt{\tau(1/a-\tau)}}, \quad (6.9)$$

where

$$\mathcal{F}_*(\zeta, u; \tau) = \left( \frac{(\zeta - \zeta_0)\sqrt{\tau}}{1 - \tau\zeta_0} - \frac{u(\zeta)(1 - \tau\zeta_0)}{i\sqrt{(1-\tau)(1-m\tau)}(\zeta - \zeta_0)} \right) \frac{\sqrt{1/a-\tau}}{(1-\tau\zeta)X^+(1/\tau, v^-)}, \quad (6.10)$$

where  $v^- = u(\xi - i0)$ . This integral is efficiently evaluated by the Gauss quadrature formulas used in (6.3), where  $m$  and  $\mathcal{F}_1$  need to be replaced by  $a$  and  $\mathcal{F}_*$ , respectively.

In the case  $\zeta \in l'_0 = (a, +\infty)^-$  on the upper sheet, the integral  $\Psi(\zeta, u)$  is singular. We denote  $u^- = u(\zeta)$ ,  $\zeta \in l'_0$ , and by the Sokhotski-Plemelj formulas,

$$\Psi^+(\zeta, u^-) = \frac{\pi - \alpha}{X^+(\zeta, u^-)} + \Psi(\zeta, u^-), \quad \zeta \in l'_0. \quad (6.11)$$

We again use the formula [1] for the Cauchy principal value  $\Psi(\zeta, u^-)$  and similar to the integral  $\mathcal{J}_1$  obtain

$$\Psi(\zeta, u^-) = \frac{\pi - \alpha}{2\pi i} \int_0^{1/a} \frac{\mathcal{F}(\tau) d\tau}{\sqrt{\tau(1/a - \tau)}(\tau - t)} = -i(\pi - \alpha)a \sum_{s=1}^{\infty} d_s U_{s-1} \left( \frac{2a}{\zeta} - 1 \right), \quad (6.12)$$

where  $t = 1/\zeta$ ,  $\zeta \in l'_0$ ,

$$\begin{aligned} \mathcal{F}(\tau) &= \left[ \frac{(1 - t\zeta_0)\sqrt{\tau}}{1 - \tau\zeta_0} + \sqrt{\frac{t(1-t)(1-mt)}{(1-\tau)(1-mt)}} \frac{1 - \tau\zeta_0}{1 - t\zeta_0} \right] \frac{\sqrt{1/a - \tau}}{X^+(1/\tau, v^-)}. \\ d_s &\approx \frac{2}{n} \sum_{j=1}^n \mathcal{F} \left( \frac{1 + x_j}{2a} \right) \cos \left( j - \frac{1}{2} \right) \frac{s\pi}{n}, \quad s = 1, 2, \dots \end{aligned} \quad (6.13)$$

Note that according to (4.55) the series in (6.12) has a logarithmic singularity as  $\zeta \rightarrow \infty$ .

The third function in the representation (4.43) of the solution of the Riemann-Hilbert problem, the function  $\Omega(\zeta, u)$ , has three real constants  $M_0$ ,  $M_1$ , and  $M_2$ . The constant  $M_2$  is the integral

$$M_2 = -\frac{\pi - \alpha}{4\pi} \int_{l'_0} \frac{d\xi}{v^- X^+(\xi, v^-)} = -\frac{\pi - \alpha}{4\pi i} \int_0^{1/a} \frac{\mathcal{F}_0(\tau) d\tau}{\sqrt{\tau(1/a - \tau)}}, \quad (6.14)$$

where

$$\mathcal{F}_0(\tau) = \frac{\sqrt{1/a - \tau}}{\sqrt{(1 - \tau)(1 - m\tau)} X^+(1/\tau, v^-)}. \quad (6.15)$$

This integral is evaluated numerically by the Gauss quadrature rule employed before.

Having equipped with formulas for  $\Phi^+(\xi, u)$  efficient for numerical purposes, we can evaluate the integrals (5.10) by applying the Gauss quadratures and solve the transcendental equation (5.9).

In the next step of the procedure we show that the conformal map we found indeed maps the contours  $l'_0$  and  $l''_0 = l_0 \setminus l'_0$  into the sides  $\arg z = \alpha$  and  $\arg z = 0$  of the wedge, respectively. Let  $\zeta \in l_0^\pm$ . Then

$$f(\zeta) = \pm \int_a^\zeta \frac{N_0 + N_1 \xi}{\sqrt{|p(\xi)|}} e^{-i\Phi^+(\xi, v^\pm)} d\xi. \quad (6.16)$$

Notice that on both sides  $l_0^\pm$  of the contour  $l_0$ ,  $\operatorname{Re} X^+(\xi, v^\pm) = 0$ ,  $\operatorname{Im} \Omega(\xi, u^\pm) = 0$ . Owing to formula (6.11), we discover

$$\Phi^+(\xi, v^-) = \pi - \alpha + iP(\xi, v^-), \quad \xi \in l'_0, \quad (6.17)$$

and for  $\xi \in l''_0$ ,

$$\Phi^+(\xi, v^+) = iP(\xi, v^+), \quad \xi \in l_0^+, \quad \Phi^+(\xi, v^-) = iP(\xi, v^-), \quad \xi \in [m, a]^-. \quad (6.18)$$

Here,

$$P(\xi, v^\pm) = \operatorname{Im} X^+(\xi, v^\pm) [\Psi(\xi, v^\pm) + \Omega(\xi, v^\pm)], \quad \xi \in l_0^\pm, \quad (6.19)$$



are real-valued functions. Returning to equation (6.16), we deduce

$$f(\zeta) = e^{i\alpha} \int_a^\zeta \frac{N_0 + N_1\xi}{\sqrt{|p(\xi)|}} e^{P(\xi, v^-)} d\xi, \quad \zeta \in l'_0,$$

$$f(\zeta) = \int_a^\zeta \frac{N_0 + N_1\xi}{\sqrt{|p(\xi)|}} e^{P(\xi, v^+)} d\xi, \quad \zeta \in l_0^+, \quad f(\zeta) = \int_a^\zeta \frac{N_0 + N_1\xi}{\sqrt{|p(\xi)|}} e^{P(\xi, v^-)} d\xi, \quad \zeta \in [m, a]^-. \quad (6.20)$$

Our numerical tests show that for the real constants  $N_0$  and  $N_1$  determined by formulas (5.11) the function  $N_0 + N_1\xi$  is positive for all  $\xi \in (m, +\infty)$ . This implies that  $z = f(\zeta)$  maps the contour  $l'_0$  into the upper side  $AB$  of the wedge, whilst the rest of the contour  $l_0^-$ ,  $[m, a]^+$ , and the upper side  $l_0^+$  of the contour  $l_0$  are mapped onto the segments  $AE$  and  $EC$  which form the whole lower side of the wedge. Here,  $E$  is the image of the point  $\zeta = m$ .

Finally, we shall let a point  $\zeta$  start at the point  $a$ , get straight to the point  $m$  first, then come to the point  $\zeta = 1$  along the straight segment, and trace both sides of the the contour  $l_1$ . The images  $z = f(\zeta)$  when  $\zeta \in l_1^\pm$  form the boundary of the hollow vortex. We have

$$f(\zeta) = H_0 + H_1 + H_2 + H^\pm(\zeta), \quad \zeta \in l_1^\pm, \quad (6.21)$$

where

$$H_0 = \int_a^m \omega_0(\xi) e^{-i\Phi^+(\xi, v^-)} d\xi, \quad H_1 = \int_m^1 \omega_0(\xi) e^{-i\Phi(\xi, v)} d\xi,$$

$$H_2 = \int_1^0 \omega_0(\xi) e^{-i\Phi^+(\xi, v^+)} d\xi, \quad H^\pm(\zeta) = \int_0^\zeta \omega_0(\xi) e^{-i\Phi^+(\xi, v^\pm)} d\xi, \quad \zeta \in l_1^\pm. \quad (6.22)$$

To evaluate these nonsingular integrals, we apply again the Gauss integration formulas with Chebyshev abscissas  $x_j = \cos(j - \frac{1}{2})\frac{\pi}{n}$ ,

$$H_0 \approx \frac{\pi}{n} \sum_{j=1}^n E_0 \left( \frac{a+m}{2} + \frac{a-m}{2} x_j \right), \quad H_1 \approx \frac{\pi i}{n} \sum_{j=1}^n E_1 \left( \frac{m+1}{2} + \frac{m-1}{2} x_j \right),$$

$$H_2 \approx \frac{\pi}{n} \sum_{j=1}^n E_2 \left( \frac{x_j+1}{2} \right), \quad H^\pm(\zeta) \approx \mp \frac{\pi}{n} \sum_{j=1}^n E^\pm \left( \frac{1+\xi_j}{2} \zeta \right). \quad (6.23)$$

Here,

$$E_0(\xi) = \sqrt{\frac{a-\xi}{\xi(\xi-1)}} (N_0 + N_1\xi) e^{-i\Phi^+(\xi, v^-)}, \quad E_1(\xi) = \frac{N_0 + N_1\xi}{\sqrt{\xi}} e^{-i\Phi(\xi, v)},$$

$$E_2(\xi) = \frac{N_0 + N_1\xi}{\sqrt{m-\xi}} e^{-i\Phi^+(\xi, v^+)}, \quad E^\pm(\xi) = \sqrt{\frac{\zeta-\xi}{(1-\xi)(m-\xi)}} (N_0 + N_1\xi) e^{-i\Phi^+(\xi, v^\pm)}. \quad (6.24)$$

For numerical tests, we select  $\zeta_0 = -5$ ,  $\delta = -3$ , and  $\eta_1 = i$ . In the case  $m = 1.5$ , the output of the Jacobi inversion problem is  $n_a = n_b = 0$  and  $\zeta_1 = 0.13498 - 1.00474i \in \mathbb{C}_1$ . For all other values of the parameters we tested, the situation is similar:  $n_a = n_b = 0$  and  $\zeta_1 \in \mathbb{C}_1$  with  $\text{Im } \zeta_1 < 0$ . In the case  $\alpha = \pi$ , the transcendental equation does not have a solution, and a hollow vortex does not exist in a half-plane. If  $\alpha \in (0, \pi)$  or  $\alpha \in (\pi, 2\pi]$ , for the values of the parameters  $m$  and  $\alpha$  tested, the transcendental equation (5.9) has a unique solution. When  $m = 1.5$  and  $\alpha = \pi/4$ , we have  $a = 1.5008430$ . As  $1 < m < 1.2$  or  $1.65 < m < 6$ , the point  $a$  becomes very close to the endpoint  $m$  of the semi-infinite contour  $l_0$ , and the numerical computations require a higher precision.

In Figures 3 to 5 we take  $\Gamma/U = 0.1$  and reconstruct the wedge and the hollow vortex boundaries on the basis of formulas (6.20) and (6.21). Figures 3 and 4 display them when  $\alpha = \pi/4$ ,  $m = 1.5$  and  $\alpha = 7\pi/4$ ,  $m = 1.2$ , respectively. In the case  $\alpha = \pi/4$ ,  $m = 1.5$  (Fig. 3), the images of the

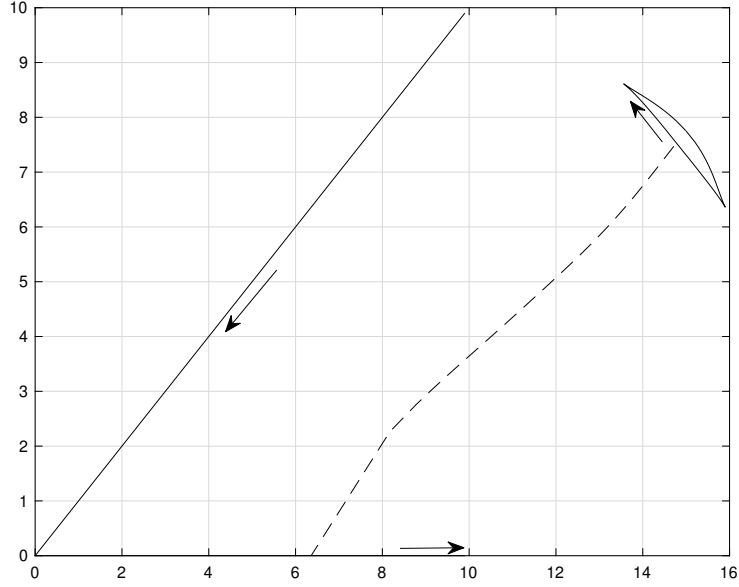


Figure 3: The hollow vortex, the wedge, and the image of the segment  $[m, 1]$  (the broken line) when  $\alpha = \pi/4$ ,  $\Gamma/U = 0.1$ ,  $m = 1.5$ .

paths  $[a, m]^-$  and  $[m, 1]$  are indicated by a solid and broken lines, respectively, with  $f(m) = 6.31$  and  $f(1) = 14.78 + 7.53i$ . At the points  $z = 15.85 + 6.36i$  and  $z = 13.51 + 8.61i$ , the images of the points  $\zeta^+ = 0.57 + i0 \in l_1^+$  and  $\zeta^- = 0.57 - i0 \in l_1^-$ , the streamline that describes the vortex boundary has cusps, and the velocity changes its direction. On comparing Figures 3 and 4 we see that for convex wedges, the closest to the wedge vertex facet of the hollow vortex is flat, while in the case  $\alpha > \pi$ , the situation is different. It is also found that for concave wedges, the hollow vortex is closer to the wedge vertex than in the case of convex wedges.

Fig. 5 illustrates the results of computations for some other values of the parameter  $m$  and the angle  $\alpha$ . In Figures 5a and 5b we display the effect of the parameter  $m$  in the case of a right-angled wedge by selecting  $m = 1.2$  in the former case and  $m = 7$  for Fig. 5b. The hollow vortex boundary is plotted for  $\alpha = 5\pi/4$  and  $m = 1.3$  in Fig. 5c. When  $\alpha \rightarrow \pi \pm 0$ , then the hollow vortex tends to be a segment and completely disappears when  $\alpha = \pi$ . Fig. 5d shows the hollow vortex shape for  $m = 1.5$  in the case of flow around a rigid semi-infinite plate  $\{0 \leq x < \infty, y = 0^\pm\}$  that is when  $\alpha = 2\pi$  (as before, the positive direction of flow around the plate and the vortex is chosen such that when a particle moves along the boundary, the flow domain is on the left).

## 7 Conclusions

Two-dimensional flow of an inviscid incompressible fluid in a wedge with impenetrable walls about a hollow vortex has been investigated by the method of conformal mappings. The map has been constructed by solving a symmetric Riemann-Hilbert problem on a finite and a semi-infinite segments lying on an elliptic Riemann surface. It turns out that owing to the asymptotics at infinity of the classical Weierstrass analogue of the Cauchy kernel for an elliptic surface and the right hand-side of the Riemann-Hilbert problem, the use of the Weierstrass kernel leads to divergent integrals. A new analogue of the Cauchy kernel on an elliptic surface with properties required has been proposed and a closed-form solution to the Riemann-Hilbert problem has been constructed. It is noted that the Weierstrass kernel would have worked if another map from the exterior of two finite segments on the flow domain had been applied. However, the authors' efforts to numerically implement

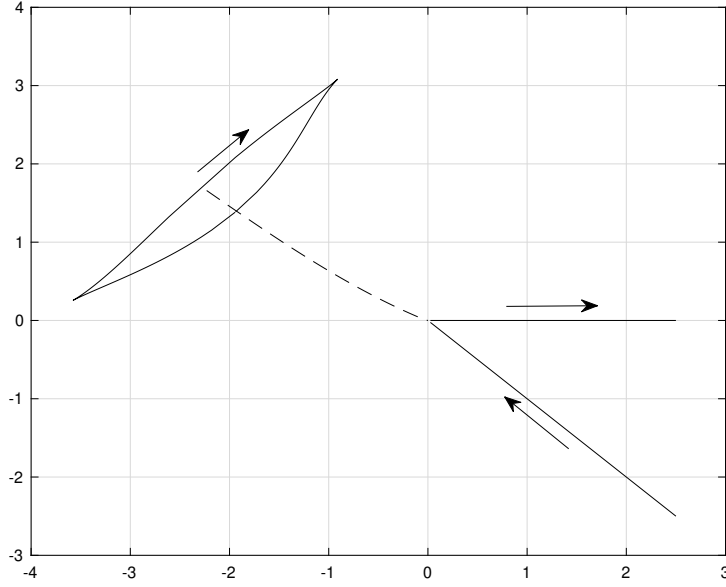


Figure 4: The hollow vortex, the wedge, and the image of the segment  $[m, 1]$  (the broken line) when  $\alpha = 7\pi/4$ ,  $\Gamma/U = 0.1$ ,  $m = 1.2$ .

the procedure and recover such a map failed. On the contrary, the mapping from a finite and a semi-infinite two-sided segments onto the hollow vortex and the wedge boundaries, respectively, has been numerically successful. A one-parametric family of such conformal mappings has been discovered in a closed-form. The hollow vortex and the wedge boundaries have been determined by quadratures and numerically reconstructed. The vortex boundaries in all numerical tests share the same feature of having two cusps at which the velocity abruptly changes its direction.

On the basis of the results shown, further extensions appear warranted. These include (i) the investigation of the stability of the flow in a wedge about a hollow vortex, (ii) the solution of the model problem of several hollow vortices in a wedge, and (iii) the consideration of the problem of a hollow vortex in a wedge with porous walls.

**Acknowledgments.** The authors thank S.G. Llewellyn Smith for drawing their attention to the problem and the Isaac Newton Institute for Mathematical Sciences, Cambridge, for support and hospitality during the program Complex analysis: techniques, applications and computations, where a part of work on this paper was undertaken.

## References

- [1] Y.A. ANTIPOV, *Method of Riemann surfaces for an inverse antiplane problem in an  $n$ -connected domain*, Complex Var. Elliptic Equ., **65** (2020), pp. 455-480.
- [2] Y.A. ANTIPOV AND V.V. SILVESTROV, *Method of Riemann surfaces in the study of supercavitating flow around two hydrofoils in a channel*, Phys. D, **235** (2007), pp. 72-81.
- [3] Y.A. ANTIPOV AND V.V. SILVESTROV, *Double cavity flow past a wedge*, Proc. R. Soc. A., **464** (2008), pp. 3021-3038.
- [4] Y.A. ANTIPOV AND A.Y. ZEMLYANOVA, *Motion of a yawed supercavitating wedge beneath a free surface*, SIAM J. Appl. Math., **70** (2009), pp. 923-948.

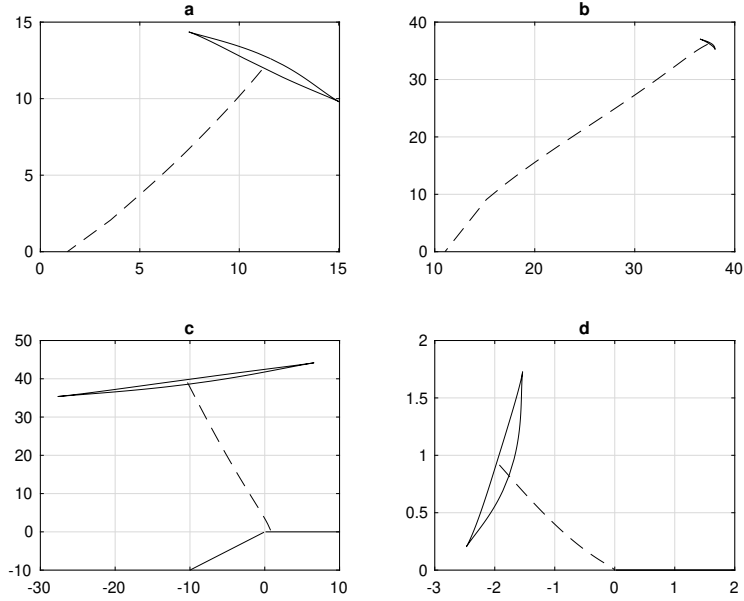


Figure 5: The hollow vortex, the wedge, and the image of the segment  $[m, 1]$  (the broken line) for  $\Gamma/U = 0.1$  when (a)  $\alpha = \pi/2$ ,  $m = 1.2$ , (b)  $\alpha = \pi/2$ ,  $m = 7$ , (c)  $\alpha = 5\pi/4$ ,  $m = 1.3$ , and (d)  $\alpha = 2\pi$ ,  $m = 1.5$ .

- [5] Y.A. ANTIPOV AND A.Y. ZEMLYANOVA, *Single- and double-spiral-vortex models for a supercavitating non-symmetric wedge in a jet*, Proc. R. Soc. A., **465** (2009), pp. 3817-3837.
- [6] K. ARDALAN, D.I. MEIRON, AND D.I. PULLIN, *Steady compressible vortex flows: the hollow-core vortex array*, J. Fluid Mech. **301** (1995), pp. 1-17.
- [7] G.R. BAKER, *Energetics of a linear array of hollow vortices of finite cross-section*, J. Fluid Mech., **99**(1) (1980), pp. 97-100.
- [8] G.R. BAKER, P.G. SAFFMAN, AND J.S. SHEFFIELD, *Structure of a linear array of hollow vortices of finite cross-section*, J. Fluid Mech., **74**(3) (1976), pp. 469-476.
- [9] J. BURBEA, *On patches of uniform vorticity in a plane of irrotational flow*, Arch. Rat. Mech. Anal., **77** (1981), pp. 349-358.
- [10] D.G. CROWDY, C.C. GREEN, *Analytical solution for von Karman streets of hollow vortices*, Phys. Fluids, **23** (2011), 126602.
- [11] D.G. CROWDY, S.G. LLEWELLYN SMITH, D.V. FREILICH, *Translating hollow vortex pairs*, Eur. J. Mech. B Fluids, **37** (2013), pp. 180-186.
- [12] M.R. DHANAK, *Stability of a regular polygon of finite vortices*, J. Fluid Mech., **234** (1992), pp. 297-316.
- [13] D.G. DRITSCHEL, *The stability and energetics of corotating uniform vortices*, J. Fluid Mech., **157** (1985), pp. 95-134.
- [14] A. ELCRAT, L. ZANNETTI, *Models for inviscid wakes past a normal plate*, J. Fluid Mech., **708** (2012), pp. 377-396.
- [15] C.C. GREEN, *Analytical solutions for two hollow vortex configurations in an infinite channel*, Eur. J. Mech. B Fluids, **54** (2015), pp. 69-81.

- [16] M.A. LAVRENTIEV, *Variational Methods for Boundary Value Problems for Systems of Elliptic Functions*, Noordhoff, 1962.
- [17] F.G. LEPPINGTON, *The field due to a pair of line vortices in a compressible fluid*, J. Fluid Mech., **559** (2006), pp. 45-55.
- [18] A. LIN, L. LANDWEBER, *On a solution of the Lavrentiev wake model and its cascade*, J. Fluid Mech., **79** (1977), pp. 801-823.
- [19] A.R. LOW, *Normal Elliptic Functions*, University of Toronto Press, Toronto, 1950.
- [20] J.H. MICHELL, *On the theory of free stream lines*, Philos. Trans. R. Soc. Lond. A, **182** (1890), pp. 394-431.
- [21] D.W. MOORE, D.I. PULLIN, *The compressible vortex pair*, J. Fluid Mech., **185** (1987), pp. 171-204.
- [22] D.W. MOORE, P.G. SAFFMAN, S. TANVEER, *The calculation of some Batchelor flows: the Sadovskii vortex and rotational corner flow*, Phys. Fluids, **31** (1988), pp. 978-990.
- [23] H.C. POCKLINGTON, *The configuration of a pair of equal and opposite hollow straight vortices, of finite cross-section, moving steadily through fluid*, Proc. Cambridge Philos. Soc., **8** (1895), 178-187.
- [24] V.S. SADOVSKII, *Vortex regions in a potential stream with a jump of Bernoulli's constant at the boundary*, Appl. Math. Mech., **35** (1971), pp. 729-735.
- [25] P.G. SAFFMAN, *Vortex Dynamics*, Cambridge University Press, Cambridge, 1992.
- [26] P.G. SAFFMAN, J.C. SCHATZMAN, *Properties of a vortex street of finite vortices*, SIAM J. Sci. Stat. Comput., **2** (1981), pp. 285-295.
- [27] P.G. SAFFMAN, R. SZETO, *Structure of a linear array of uniform vortices*, Stud. Appl. Math., **65** (1981), pp. 223-248.
- [28] S.G. LLEWELLYN SMITH, D.G. CROWDY, *Structure and stability of hollow vortex equilibria*, J. Fluid Mech., **691** (2012), pp. 170-200.
- [29] H. TELIB, L. ZANNETTI, *Hollow wakes past arbitrarily shaped obstacles*, J. Fluid Mech., **669** (2011), pp. 214-224.
- [30] L. ZANNETTI, M. FERLAUTO, S.G. LLEWELLYN SMITH, *Hollow vortices in shear*, J. Fluid Mech., **809** (2016), pp. 705-715.
- [31] L. ZANNETTI, D. LASAGNA, *Hollow vortices and wakes past Chaplygin cusps*, Eur. J. Mech. B Fluids, **38** (2013), pp. 78-84.
- [32] A.Y. ZEMLYANOVA AND Y.A. ANTIPOV, *Single-spiral-vortex Model for a Cavitating Elastic Curvilinear Foil*, SIAM J. Appl. Math., **72** (2012), pp. 280-298.
- [33] E. I. ZVEROVICH, *Boundary value problems in the theory of analytic functions in Hölder classes on Riemann surfaces*, Russian Math. Surveys, **26** (1971), pp. 117-192,